

Dark matter from late invisible decays to and of gravitinosRouzbeh Allahverdi,¹ Bhaskar Dutta,² Farinaldo S. Queiroz,³ Louis E. Strigari,² and Mei-Yu Wang²¹*Department of Physics and Astronomy, University of New Mexico, Albuquerque, New Mexico 87131, USA*²*Department of Physics and Astronomy, Mitchell Institute for Fundamental Physics and Astronomy, Texas A & M University, College Station, Texas 77843-4242, USA*³*Department of Physics and Santa Cruz Institute for Particle Physics, University of California, Santa Cruz, California 95064, USA*

(Received 26 December 2014; published 30 March 2015)

In this work, we sift a simple supersymmetric framework of late invisible decays to and of the gravitino. We study a simple extension of the minimal supersymmetric standard model that includes isosinglet color-triplet superfields and a singlet superfield. We investigate two cases where the gravitino is the lightest supersymmetric particle or the next-to-lightest supersymmetric particle. The next-to-lightest supersymmetric particle decays into two dark matter candidates and has a long lifetime due to gravitationally suppressed interactions. However, because of the absence of any hadronic or electromagnetic products, it satisfies the tight bounds set by big bang nucleosynthesis and the cosmic microwave background. One or both of the dark matter candidates produced in invisible decays can contribute to the amount of dark radiation and suppress perturbations at scales that are being probed by the galaxy power spectrum and the Lyman-alpha forest data. We show that these constraints are satisfied in large regions of the parameter space and, as a result, the late invisible decays to and of the gravitino can be responsible for the entire dark matter relic abundance.

DOI: [10.1103/PhysRevD.91.055033](https://doi.org/10.1103/PhysRevD.91.055033)

PACS numbers: 12.60.Jv, 12.60.-i, 95.30.Cq

I. INTRODUCTION

There are various lines of evidence for the existence of dark matter (DM) in the Universe [1], but its identity is still unknown and remains one of the most important problems at the interface of cosmology and particle physics. Given the many ongoing direct and indirect DM detection experiments, along with collider searches trying to pin down the nature of DM, this puzzle should be solved in the foreseeable future.

Supersymmetric (SUSY) extensions of the standard model (SM) with R -parity conservation provide a natural candidate for DM. In these models, the lightest supersymmetric particle (LSP) is stable and hence can account for the DM particle. In the minimal supersymmetric standard model (MSSM), the LSP is either the lightest neutralino $\tilde{\chi}_1^0$ or the gravitino \tilde{G} .

The presence of the gravitino results in important cosmological constraints on SUSY models. If the gravitino is not the LSP, then it will decay to the LSP and its SUSY partner. If the gravitino is the LSP, then the next-to-lightest supersymmetric particle (NLSP) will decay to the gravitino. Because of Planck suppressed interactions of \tilde{G} with other particles [2], these decays have long lifetimes. In particular, if $m_{\tilde{G}} < 40$ TeV, the decay to and of the gravitino will occur after the onset of big bang nucleosynthesis (BBN). Such decays are tightly constrained by cosmological considerations from BBN and the cosmic microwave background (CMB). Late decays of neutral or charged particles through electromagnetic and hadronic

channels are severely restricted by BBN constraints [3,4]. Moreover, late decays that release energy in the electromagnetic mode can give rise to a chemical potential for the CMB photons [5,6] which is constrained by observations [7]. A late injection of energetic neutrinos, which can produce secondary particles, is constrained by BBN bounds as well as CMB limits on the amount of extra radiation and structure formation [8]. These bounds severely constrain the abundance of the NLSP and, through that, put tight limits on the reheating of the Universe. These studies in the context of axion/axino production from invisible decays have been discussed in Ref. [9]. For other recent dark radiation setups see Ref. [10].

In this paper, we investigate a SUSY scenario that can accommodate invisible decay to and of the gravitino. The model is a minimal extension of the MSSM and has two DM candidates. One of the DM candidates is the LSP and the other one is an R -parity even fermion N with an $\mathcal{O}(\text{GeV})$ mass that is a singlet under the SM gauge group. The LSP in this model can be either the gravitino or the SUSY partner of N (denoted by \tilde{N}). The model is well motivated due to its ability to generate the baryon abundance of the Universe at temperatures well below the electroweak scale, and to explain the apparent coincidence between the observed DM and baryon energy densities [11,12]. The invisible decays involving the gravitino are $\tilde{N} \rightarrow \tilde{G} + N$ and $\tilde{G} \rightarrow \tilde{N} + N$, which, respectively, take place for a gravitino NLSP and an \tilde{N} NLSP and vice versa. Although both decays involve gravitationally suppressed interactions, and hence

have a long lifetime, they circumvent the severe BBN and CMB constraints since they do not include electromagnetic or hadronic products.

However, depending on the mass ratio between \tilde{N} and \tilde{G} , it is possible that one or both of the decay products are relativistic during the epoch of matter-radiation equality. They may then contribute to the amount of dark radiation and suppress DM perturbation scales that are probed by the galaxy clustering and the Lyman-alpha forest data. We will show that for the current data these constraints are satisfied in large regions of the parameter space. As a result, the late decays can be responsible for the entire DM relic abundance in this model. Moreover, in a broader context, late invisible decays to and of the gravitino considerably relax the constraints on the reheating of the Universe in SUSY models [13].

The structure of this paper is as follows. In Sec. II, we discuss the model. In Sec. III, we discuss the late invisible decays that involve the gravitino. We discuss production of dark radiation in Sec. IV, and constraints from structure formation in Sec. V. We present our results in Sec. VI. Finally, we close this paper by concluding it in Sec. VII.

II. THE MODEL

The model is an extension of the MSSM that contains isosinglet color-triplet superfields X and \bar{X} with respective hypercharges $+4/3$ and $-4/3$, and a singlet superfield N . The superpotential of this model is given by [14]

$$W = W_{\text{MSSM}} + W_{\text{new}},$$

$$W_{\text{new}} = \lambda_i X N u_i^c + \lambda'_{ij} \bar{X} d_i^c d_j^c + M_X X \bar{X} + \frac{M_N}{2} N N. \quad (1)$$

Here i, j denote flavor indices (color indices are omitted for simplicity), with λ'_{ij} being antisymmetric under $i \leftrightarrow j$. We assign quantum number $+1$ under R parity to the scalar components of X, \bar{X} and the fermionic components of N . As shown in [11,12,14], with two (or more) copies of X, \bar{X} , one can generate the baryon asymmetry of the Universe from the interference of tree-level and one-loop diagrams in decay processes governed by the X, \bar{X} interactions.

The exchange of X, \bar{X} particles in combination with the Majorana mass of N leads to the double proton decay $pp \rightarrow K^+ K^+$. Current limits on this process from the Super-Kamiokande experiment [15] require that $|\lambda_i \lambda'_{12}|^2 \leq 10^{-10}$ for $M_N \sim 100$ GeV. This is also enough to satisfy constraints from $K_s^0 - \bar{K}_s^0$ and $B_s^0 - \bar{B}_s^0$ mixing and neutron-antineutron oscillations [11].

Assuming that $M_N \ll M_X$, one finds an effective four-fermion interaction $N u_i^c d_j^c d_k^c$ after integrating out the scalars $\tilde{X}, \tilde{\bar{X}}$. This results in decay modes $N \rightarrow p + e^- + \bar{\nu}_e$, $N \rightarrow \bar{p} + e^+ + \nu_e$, which are kinematically open as long as $M_N > m_p + m_e$ (with m_p and m_e being the proton mass and the electron mass, respectively). It is seen

that N becomes absolutely stable if $M_N \leq m_p + m_e$. However, in this case, we will have catastrophic proton decay via $p \rightarrow N + e^+ + \nu_e$ if $m_p > M_N + m_e$. Therefore a viable scenario with stable N arises, provided that

$$m_p - m_e \leq M_N \leq m_p + m_e. \quad (2)$$

The important point to emphasize is that the stability of N is not related to any new symmetry. It is the stability of the proton, combined with the kinematic condition in Eq. (2), that ensures that N is a stable particle in the above mass window. This leads to a natural realization of GeV DM with or without SUSY [16], which provides a suitable framework to address the DM-baryon coincidence puzzle. Possible signatures of such an $\mathcal{O}(\text{GeV})$ GeV DM particle in collider and indirect searches have been studied in [17,18].

When R parity is conserved, which we assume to be the case here, the LSP is also a DM candidate. Consequently, if $M_N \approx \mathcal{O}(\text{GeV})$, a multicomponent DM scenario can be realized in this model, as both the LSP and N are stable in this case.

After SUSY breaking, the real and imaginary parts of \tilde{N} acquire different masses:

$$m_{\tilde{N}_{1,R}}^2 = M_N^2 + \tilde{m}^2 \mp B_N M_N, \quad (3)$$

where \tilde{m} is the soft SUSY breaking mass of \tilde{N} and $B_N M_N$ is the B term associated with the $M_N N^2/2$ superpotential term. Depending on the sign of B_N , \tilde{N}_R or \tilde{N}_I will be the lighter of the two mass eigenstates. In the special case that $|B_N M_N| \ll \tilde{m}^2$, \tilde{N}_R and \tilde{N}_I are approximately degenerate. It is clear that there are regions in the parameter space where \tilde{N} (or one of its components) is either the LSP or the NLSP. As we will show below, particularly interesting scenarios can arise with the \tilde{N} LSP and the gravitino NLSP and vice versa.

Before closing this section, we briefly comment on the prospects for the detection of N and \tilde{N} as DM candidates in this model. N interacts with nucleons via its coupling to the up quark that is mediated by the X scalar; see Eq. (1). The resulting spin-independent scattering cross section is extremely small, as pointed out in [16]. The spin-dependent scattering cross section is $\sigma_{N-p}^{\text{SD}} \sim |\lambda|^2 m_p^2 / 64 \pi m_X^4$ [16], where m_X denotes the mass of the X scalar. For $m_X \sim \mathcal{O}(\text{TeV})$ and $|\lambda| \sim 1$, we have $\sigma_{N-p}^{\text{SD}} \sim 10^{-42}$ cm². This is much below the current bounds from direct detection experiments [19], but within the LHC future reach [20]. The situation is more promising for \tilde{N} . It interacts with nucleons via an exchange of the X fermion with up quarks, which results in a spin-independent scattering cross section $\sigma_{\tilde{N}-p}^{\text{SI}} \sim |\lambda|^2 m_p^2 / 16 \pi M_X^4$ [14]. For $M_X \sim \mathcal{O}(\text{TeV})$ and $|\lambda|^{-1} \leq 10^{-1}$, we have $\sigma_{\tilde{N}-p}^{\text{SI}} < 10^{-45}$ cm², which is

well within the range currently being probed by direct detection searches [21].

III. LATE INVISIBLE DECAYS

As mentioned earlier, late decays that involve the gravitino are subject to very tight cosmological constraints from BBN and CMB [3–8]. Interestingly, however, the model given in Eq. (1) can result in invisible decays to and of the gravitino, thereby circumventing these tight cosmological constraints.¹ The two interesting scenarios, pointed out before, are (1) \tilde{N} NLSP and gravitino LSP, and (2) \tilde{N} LSP and gravitino NLSP. The decays $\tilde{N} \rightarrow \tilde{G} + N$ (in the former case) and $\tilde{G} \rightarrow \tilde{N} + N$ (in the latter case) do not produce charged particles, hadrons, or neutrinos.² They are therefore totally invisible and, as a result, evade the above BBN and CMB bounds. We note, however, that these decays can produce relativistic DM quanta. Cosmological constraints on the model then come from the effective number of neutrinos N_{eff} and from structure formation, which we will discuss in detail later on.

Here we describe different possibilities for a late invisible decay that can arise in our model in more detail:

- (1) \tilde{N} NLSP and gravitino LSP, $m_{\tilde{N}} > M_N \gg m_{\tilde{G}}$. The late decay is $\tilde{N} \rightarrow \tilde{G} + N$ with the corresponding width

$$\Gamma_{\tilde{N} \rightarrow N + \tilde{G}} = \frac{1}{48\pi} \frac{m_{\tilde{N}}^5}{M_{\text{P}}^2 m_{\tilde{G}}^2} \left(1 - \frac{M_N^2}{m_{\tilde{N}}^2}\right)^4. \quad (4)$$

For $M_N \approx 1$ GeV, which we consider here, both of the decay products are stable and contribute to the DM relic abundance. However, since $m_{3/2} \ll \mathcal{O}(\text{GeV})$, the contribution of the gravitino is subdominant. In this case, the dominant component of DM is N , while relativistically produced gravitinos from \tilde{N} decay may contribute to the dark radiation. Gravitinos much lighter than GeV can be realized in models of gauge-mediated SUSY breaking. We note that such light gravitinos do not affect the stability of N , as the only R -parity conserving decay mode $N \rightarrow \tilde{G} \tilde{G}$ is forbidden by Lorentz invariance.

- (2) \tilde{N} NLSP and gravitino LSP, $m_{\tilde{N}} > m_{\tilde{G}} \gg M_N$. The late decay is $\tilde{N} \rightarrow \tilde{G} + N$ and the corresponding decay width is

¹Invisible decays of and to gravitinos involving axino and axion have been discussed in [22].

²Secondary production of these particles from the interaction of N and \tilde{N} with nucleons is totally negligible since the corresponding cross section is several orders of magnitude smaller than that of the weak interactions for typical values of the model parameters.

$$\Gamma_{\tilde{N} \rightarrow N + \tilde{G}} = \frac{1}{48\pi} \frac{m_{\tilde{N}}^5}{M_{\text{P}}^2 m_{\tilde{G}}^2} \left(1 - \frac{m_{\tilde{G}}^2}{m_{\tilde{N}}^2}\right)^4. \quad (5)$$

Both \tilde{N} and N contribute to the DM relic density. However, since $m_{\tilde{G}} \gg \mathcal{O}(\text{GeV})$, gravitinos constitute the dominant component of DM, and relativistically produced N quanta from the decay may contribute to the dark radiation.

- (3) \tilde{G} NLSP and \tilde{N} LSP, $m_{\tilde{G}} > m_{\tilde{N}} \gg M_N$. The late decay is $\tilde{G} \rightarrow \tilde{N} + N$ and has the following decay width:

$$\Gamma_{\tilde{G} \rightarrow \tilde{N} + N} = \frac{1}{192\pi} \frac{m_{\tilde{G}}^3}{M_{\text{P}}^2} \left(1 - \frac{m_{\tilde{N}}^2}{m_{\tilde{G}}^2}\right)^4. \quad (6)$$

Both \tilde{N} and N contribute to the DM relic abundance. However, since $m_{\tilde{N}} \gg \mathcal{O}(\text{GeV})$, the dominant component of DM is \tilde{N} , while relativistically produced N quanta from the \tilde{G} decay may contribute to the dark radiation.

Since $M_N \approx 1$ GeV is set by the stability condition of N , the parameter space relevant for late decay in all three of the cases is two dimensional, namely, the $m_{\tilde{N}} - m_{\tilde{G}}$ plane. We will discuss in detail the allowed regions of the parameter space for each of these cases later on.

Some comments are in order before we close this section. Even though the late decays mentioned above are invisible, they are inevitably accompanied by higher-order processes that produce hadrons and charged particles. One notable channel, shown in Fig. 1, is NLSP decay to three quark final states mediated by an off-shell N and the X, \bar{X} scalars. The branching ratio for this mode is given by

$$\text{Br}_{\text{h}} \sim \frac{1}{(16\pi^2)^2} \cdot 3 \cdot |\lambda\lambda'|^2 \left(\frac{B_X M_X m_{\text{NLSP}}^2}{m_X^4}\right)^2. \quad (7)$$

Here $B_X M_X$ is the B term associated with the $M_X X \bar{X}$ term in Eq. (1), and we have assumed that $m_{\text{NLSP}} \gg m_{\text{LSP}}$. The

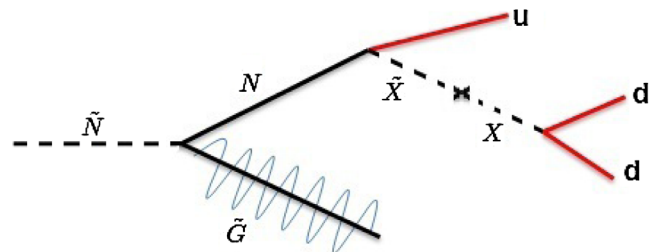


FIG. 1 (color online). The hadronic decay mode of \tilde{N} in cases 1 and 2. The branching ratio for this channel, given in Eq. (7), is typically very small and easily satisfies the tightest BBN bounds. A similar diagram exists for the hadronic decay of \tilde{G} in case 3, with the roles of \tilde{N} and \tilde{G} being reversed.

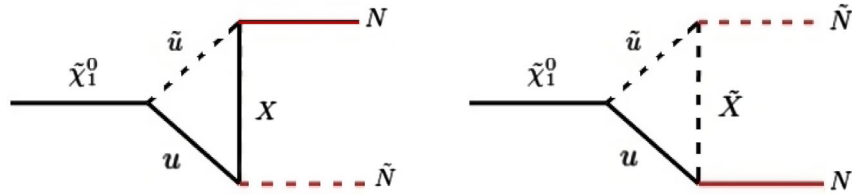


FIG. 2 (color online). Typical diagrams for the decay of a bino-type $\tilde{\chi}_1^0$ into $\tilde{N}N$. Additional diagrams that are obtained by switching $u \leftrightarrow X$ and $\tilde{u} \leftrightarrow \tilde{X}$ in the loop. The SUSY breaking contributions from the diagram on the right dominate, giving rise to the decay width in Eq. (8).

first factor on the rhs of Eq. (7) is the ratio of the phase space factors for four-body and two-body decays, respectively, and 3 denotes the color multiplicity factor. For M_X , $m_X \gtrsim \mathcal{O}(\text{TeV})$ (to be compatible with the LHC bounds on the colored particles) and $|B_X| \sim \mathcal{O}(\text{TeV})$, moderately small values of $|\lambda\lambda'|$ and $m_{\text{NLSP}} \lesssim 100$ GeV will be enough to push Br_h down below 10^{-10} . Such a small value of Br_h easily satisfies the tight constraints from the BBN and CMB bounds mentioned above [3–6,8].

Finally, there are other potentially dangerous decay modes that need to be considered. The lightest SUSY particle in the MSSM sector can decay to \tilde{N} and to the gravitino. These decays can be dangerous if the corresponding lifetime exceeds 1 second. To avoid this, it suffices if the more efficient decay takes place before the onset of BBN. The lightest SUSY particle in the MSSM sector can be the lightest neutralino $\tilde{\chi}_1^0$, the sneutrino $\tilde{\nu}$, or the slepton \tilde{l} . The neutralino $\tilde{\chi}_1^0$ undergoes two-body decay to $\tilde{N}N$ and four-body decay to $u\tilde{u}N\tilde{N}$. The two-body decay occurs via a loop diagram and is dominant. Figure 2 shows typical diagrams for the decay of a bino-type $\tilde{\chi}_1^0$. The decay width receives contributions from SUSY preserving and SUSY breaking interactions. The latter dominates by a factor of $(A_X/M_N)^2$, where A_X is the A term associated with the XNu^c superpotential term; see Eq. (1). The resulting decay width is

$$\Gamma_{\tilde{\chi}_1^0} \sim \frac{4}{3} \cdot \frac{1}{(4\pi)^4} \cdot \frac{1}{8\pi} \alpha |\lambda|^4 \frac{m_{\tilde{\chi}_1^0}^3 A_X^2}{M_X^4}. \quad (8)$$

Here α is the electroweak fine structure constant; factors of $4/3$ and $1/(4\pi)^4$ on the rhs take the color multiplicity and hypercharge of the up-type quarks and the loop factor, respectively, into account; and we have assumed that $m_{\tilde{\chi}_1^0} \gg m_{\tilde{N}}$. As mentioned before, only the combination $|\lambda\lambda'|$ is subject to phenomenological constraints in our model, and hence $|\lambda|$ does not need to be very small. For $A_X, M_X \sim 1$ TeV, $m_{\tilde{\chi}_1^0} \sim 100$ GeV, and $|\lambda| \sim 10^{-2}$, we find $\tau_{\tilde{\chi}_1^0} \ll 10^{-6}$ sec. A combination of SUSY breaking and electroweak breaking interactions leads to similar decay widths for wino-type and Higgsino-type $\tilde{\chi}_1^0$'s via one-loop

diagrams. The sneutrino $\tilde{\nu}$ and the slepton \tilde{l} decay to $\nu N\tilde{N}$ and $lN\tilde{N}$ final states via an off-shell bino, and the corresponding decay widths are still $\ll 1$ sec. We therefore see that, for a reasonable choice of parameters, the lightest SUSY particle in the MSSM sector decays early enough to easily avoid any potential danger.

IV. DARK RADIATION CONSTRAINTS ON LATE INVISIBLE DECAYS

The amount of dark radiation in the early Universe is parametrized by the effective number of neutrinos N_{eff} . The present observational bound on $\Delta N_{\text{eff}} \equiv N_{\text{eff}} - N_{\text{eff,SM}}$ (where $N_{\text{eff}} = 3.04$) from Planck + WMAP9 + ACT + SPT + BAO + HST at 2σ is $\Delta N_{\text{eff}} = 0.48_{-0.45}^{+0.48}$ [23], which implies that $\Delta N_{\text{eff}} = 0.96$ at 2σ . The precise value of N_{eff} depends on the Hubble constant where the Planck data and HST measurements differ [24]. The reconciliation can occur using a nonzero ΔN_{eff} [25]. Setting aside the dust contamination in the BICEP2 results, the tension in the CMB tensor polarization measurement between the recent BICEP2 [26] and Planck data can also be reconciled with $\Delta N_{\text{eff}} = 0.81 \pm 0.25$ at more than a 3σ confidence level in a joint analysis [27], disfavoring $\Delta N_{\text{eff}} = 0$. Since the presence of dark radiation is debatable, here we take a more conservative approach. We use the data to derive bounds on frameworks that may naturally induce a non-negligible dark radiation component through nonthermal DM production.

In order to relate the energy density associated with nonthermally, relativistically produced DM with the effective number of neutrinos, we start by calculating the ratio between their respective energy densities. Since the cold dark matter and neutrino energy densities are redshifted, like $\rho_{\text{DM}} \propto \Omega_{\text{DM}} a^{-3}$ and $\rho_\nu \propto \Omega_\nu a_{\text{eq}}^{-4} N_\nu / 3$, the ratio between the neutrino and DM energy densities at the matter-radiation equality is

$$\frac{\rho_\nu}{\rho_{\text{DM}}} = \frac{\Omega_\nu}{\Omega_{\text{DM}}} \frac{N_\nu}{3} \frac{1}{a_{\text{eq}}} = \frac{0.69 \Omega_\nu}{\Omega_{\text{DM}}} \frac{N_\nu}{3} \frac{1}{a_{\text{eq}}}, \quad (9)$$

where $\Omega_\nu \simeq 4.84 \times 10^{-5}$, $\Omega_{\text{DM}} \sim 0.227$, and N_ν is the number of neutrinos. For $N_\nu = 1$, we thus find that the energy density of one neutrino is $\sim 16\%$ of the DM density.

As a result, if DM particles had a kinetic energy equivalent to $\gamma_{\text{DM}} \approx 1.16$ at t_{eq} , this fraction would produce the same effect as an extra neutrino species in the expansion of the Universe at that time [28]. However, as we will discuss below, constraints stemming from structure formation require the fraction of DM particles with appreciable kinetic energy to be $\ll 1$. Therefore, in order to still mimic one neutrino species, a small fraction of DM particles have to be relativistically produced.

In the general decay setup where a heavy particle with mass M decays at rest to two particles with masses m_1 and m_2 at time t_{dec} , the boost factors of the daughter particles follow:

$$\begin{aligned}\gamma_1(t)^2 &= 1 + \frac{a_{\text{dec}}^2 p^2}{a^2(t) m_1^2}, \\ \gamma_2(t)^2 &= 1 + \frac{a_{\text{dec}}^2 p^2}{a^2(t) m_2^2},\end{aligned}\quad (10)$$

where

$$p = \frac{[(M^2 - (m_1 + m_2)^2)(M^2 - (m_1 - m_2)^2)]^{1/2}}{2M} \quad (11)$$

is the momentum of the daughter particles at the time of production.

If both of the daughter particles are stable, they both contribute to the DM relic density. If f is the fraction of the energy density in DM that is produced from the late decay, the amount of dark radiation that is mimicked by the kinetic energy of the daughter particles is found to be

$$\Delta N_{\text{eff}} = \left[\frac{(\gamma_{1,\text{eq}} - 1)m_1 + (\gamma_{2,\text{eq}} - 1)m_2}{0.16(m_1 + m_2)} \right] f. \quad (12)$$

We note that the above normalization factor of 0.16 appears due to the neutrino-DM energy density fraction at the matter-radiation equality found in Eq. (9).

If $m_1 \ll m_2$, then the likely scenario is that species 1 is the dominant DM component, hence $m_{\text{DM}} \approx m_1$, while species 2 makes the major contribution to the dark radiation.³ In this case, assuming that $\gamma_{2,\text{eq}} \gg 1$, we have

$$\Delta N_{\text{eff}} \approx 4.87 \times 10^{-3} \left(\frac{t_{\text{dec}}}{10^6 \text{ s}} \right)^{1/2} \left(\frac{p}{m_{\text{DM}}} \right) f, \quad (13)$$

where p is given in Eq. (11).

V. STRUCTURE FORMATION CONSTRAINTS ON LATE INVISIBLE DECAYS

In this section, we discuss large scale structure constraints and present our results for dark radiation in the

³The case where the same species is responsible for DM and dark radiation was studied in detail in [28–31].

model described in Sec. II. The median speed of the decay products at a given time t for $M \rightarrow m_1 + m_2$ is described by

$$v_{1,2,\text{med}}(t) \sim \frac{a_{\text{dec}}/a(t)p}{\sqrt{(a_{\text{dec}}/a(t)p)^2 + m_{1,2}^2}}. \quad (14)$$

The scaling of the free-streaming distance can be understood in terms of the Jeans wave number:

$$k_{\text{fs}}(a) = \frac{\sqrt{\rho a^2/2M_{\text{P}}^2}}{v_{\text{med}}(a)} = \sqrt{\frac{3}{2}} \frac{aH(a)}{v_{\text{med}}(a)}, \quad (15)$$

where, for $k > k_{\text{fs}}$, the density perturbation is suppressed.

Correlation of the galaxy distribution probes the matter power spectrum on scales of $0.02 \text{ h Mpc}^{-1} \lesssim k \lesssim 0.2 \text{ h Mpc}^{-1}$ at $z \sim 0$ [32]. Indeed, one of the best cosmological probes of constraining massive standard model neutrinos, as a class of “hot dark matter” (HDM), is the galaxy power spectrum. The current neutrino mass limits from SDSS galaxy clustering is about $\Sigma m_\nu < 0.3\text{--}0.62 \text{ eV}$ [32]. The abundance of HDM that is allowed by the current galaxy power spectrum is given by

$$\Omega_\nu h^2 = \frac{\Sigma m_\nu}{94.1 \text{ eV}}. \quad (16)$$

This predicts $\Omega_\nu \lesssim 0.007\text{--}0.01$, which gives the ratio of DM and HDM $\Omega_\nu/\Omega_{\text{DM}} \lesssim 0.03\text{--}0.06$. Therefore the amount of HDM that suppresses structure growth at scale $k \sim 0.02h \text{ Mpc}^{-1}\text{--}0.2h \text{ Mpc}^{-1}$, either from the subdominant part or the dominant part of the dark matter, is limited to be less than 3–6% of the total dark matter.

Lyman-alpha forest data probes the matter power spectrum on smaller scales, $0.1 \text{ h Mpc}^{-1} \lesssim k \lesssim 2 \text{ h Mpc}^{-1}$ at $z \sim 2\text{--}4$ [33,34]. For current Lyman-alpha forest data, the error of measurement is roughly in the range of 5%–10% [33,34]. In [35], the authors utilize numerical simulations to study Lyman-alpha forest limits for the warm + cold dark matter models. They found that, with a fraction of sterile neutrino warm dark matter (WDM) $f_{\text{WDM}} < 0.35$, any mass of WDM in the range they studied is allowed by the data. So the amount of WDM which suppresses structure growth at scale $k \sim 0.1 \text{ h Mpc}^{-1}\text{--}2 \text{ h Mpc}^{-1}$ cannot be more than 10%–35% of the total dark matter.

In Fig. 3, we plot the free-streaming scale k_{fs} for N and \tilde{G} for the decay process $\tilde{N} \rightarrow \tilde{G} + N$ (case 1) as a function of scale factor a . Each panel is for a different value of $m_{\tilde{G}}$ and $m_{\tilde{N}}$. We find that k_{fs} for the decay products, depending on the masses, can suppress scales that can be probed by the large scale structure data.

We note that constraints on our late invisible decay models from estimates of the free-streaming length are meant to provide rough estimates. To understand the power spectrum suppression scale accurately, one will need to solve the Boltzmann equations and derive the perturbation

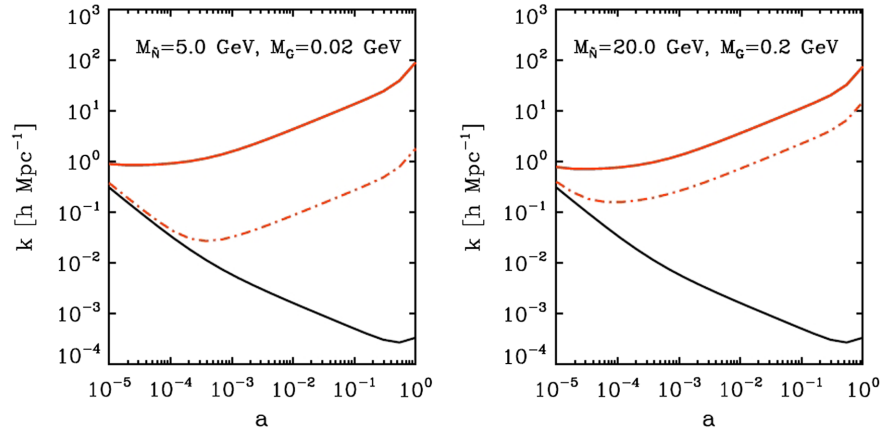


FIG. 3 (color online). The free-streaming scale k_{fs} for N and \tilde{G} for the decay process $\tilde{N} \rightarrow \tilde{G} + N$ (case 1) as a function of scale factor a . Each panel is for a different value of $m_{\tilde{G}}$ and $m_{\tilde{N}}$. For the left panel the mass is set to $m_{\tilde{N}} = 5$ GeV and $m_{\tilde{G}} = 0.02$ GeV; in the right panel masses are set to $m_{\tilde{N}} = 20$ GeV and $m_{\tilde{G}} = 0.2$ GeV. The mass of m_N is 1 GeV. The black solid line is the size of the horizon at a given scale factor. The solid color lines are for N , and the dash-dotted lines are for \tilde{G} . The density perturbation is suppressed for $k > k_{\text{fs}}$. Between k_{fs} and the horizon, the density perturbation will grow.

evolution [36,37]. However, this is beyond the scope of this study, and we will leave this for future work.

VI. RESULTS

In this section, we present our results. In Figs. 4–6, we include the constraints from structure formation and plot ΔN_{eff} in the $m_{\text{NLSP}} - m_{\text{LSP}}$ parameter space. The figures depict contours for the decay lifetime t_{dec} of the NLSP and bands representing the value of ΔN_{eff} . We have shown LSP masses up to 1 TeV; for larger masses, the SUSY particles will be too heavy to have a realistic prospect for detection at the LHC. We also note that the region $m_{\text{NLSP}} \leq m_{\text{LSP}} + M_N$, where $M_N \approx 1$ GeV, is kinematically forbidden.

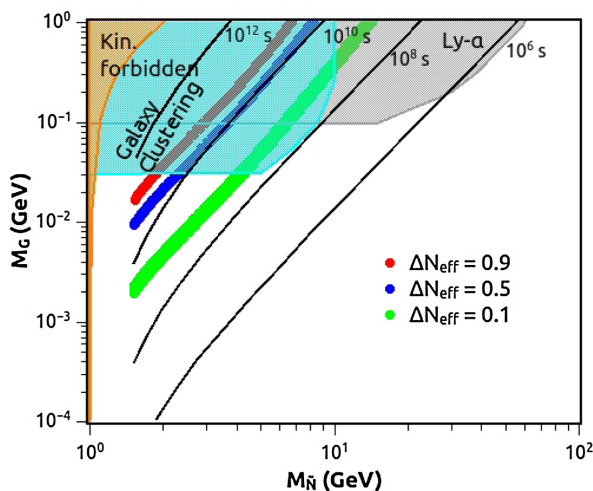


FIG. 4 (color online). The allowed region of the parameter space in case 1 ($\tilde{N} \rightarrow \tilde{G} + N$, $m_{\tilde{G}} \ll M_N \approx 1$ GeV) is shown. Lifetime contours of \tilde{N} and $\Delta N_{\text{eff}} = \text{const}$ bands are included.

Figure 4 shows the results for case 1, the $\tilde{N} \rightarrow N + \tilde{G}$ decay with $m_{\tilde{N}} > M_N \gg m_{\tilde{G}}$. In this case, N is the dominant component of DM, and gravitino quanta from the \tilde{N} decay make the main contribution to dark radiation. The corresponding decay width is given by Eq. (4), where $M_N \approx 1$ GeV. Since the decay creates the same number of N and \tilde{G} quanta, the contribution of gravitinos to the total DM density is $f m_{\tilde{G}}/1$ GeV, where f is the ratio of the N number density from the \tilde{N} decay to its total value. We take $f = 1$ henceforth, which results in the tightest bounds from structure formation and ΔN_{eff} . If we use smaller values of f , the constraints will become weaker, but we also need to have an additional source of DM.

For $m_{\tilde{N}} \gg 1$ GeV, Eqs. (4), (11), and (13) result in $\Delta N_{\text{eff}} \propto m_{\tilde{G}}/m_{\tilde{N}}^{3/2}$, implying that $\Delta N_{\text{eff}} = \text{const}$ bands lie along the curves $m_{\tilde{N}}^3 \propto \Delta N_{\text{eff}}^2 m_{\tilde{G}}^2$. We note, however, that $m_{\tilde{G}}$ eventually catches up with $m_{\tilde{N}}$, at which point the decay becomes kinematically impossible. Therefore, the $\Delta N_{\text{eff}} = \text{const}$ bands have a turning point where they bend to the left, as seen in the figure.

We find that the Lyman-alpha forest data is effective in constraining the parameter space for $m_{\tilde{N}} > 10$ GeV, while the galaxy power spectrum sets a stronger constraint for $m_{\tilde{N}} < 10$ GeV. In the latter case, the gravitino mass needs to be smaller than 0.01 GeV. We see that it is still possible to get $\Delta N_{\text{eff}} \sim 0.5$ in the allowed region of the parameter space for $m_{\tilde{N}} < 2$ GeV.

Figure 5 shows the results for case 2, the $\tilde{N} \rightarrow N + \tilde{G}$ decay with $m_{\tilde{N}} > m_{\tilde{G}} \gg M_N$. In this case, the gravitino is the dominant component of DM, and N quanta from the \tilde{N} decay make the main contribution to dark radiation. The corresponding decay width is given by Eq. (5), where $M_N \approx 1$ GeV.

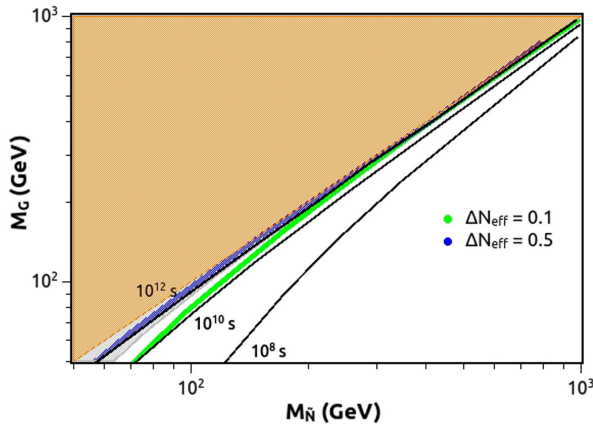


FIG. 5 (color online). The same as Fig. 4, but for case 2 ($\tilde{N} \rightarrow \tilde{G} + N$, $m_{\tilde{G}} \gg M_N \approx 1$ GeV).

Equations (5), (11), and (13) result in $\Delta N_{\text{eff}} \propto m^{1/2}/(m_{\tilde{N}}^2 - m_{\tilde{G}}^2)$. This implies that the $\Delta N_{\text{eff}} = \text{const}$ bands are concentrated around the line $m_{\tilde{N}} = m_{\tilde{G}}$ for large values of $m_{\tilde{N}}$, as seen in the figure.

We find that the Lyman-alpha forest data is effective in constraining the parameter space for $m_{\tilde{G}} > 100$ GeV, while the galaxy power spectrum sets a stronger constraint for $m_{\tilde{G}} < 100$ GeV. Combining both constraints, we find that $\Delta N_{\text{eff}} \lesssim 0.1$ in the allowed region of the parameter space.

Figure 6 shows the results for case 3, the $\tilde{G} \rightarrow \tilde{N} + N$ decay with $m_{\tilde{G}} > m_{\tilde{N}} \gg M_N$. In this case, \tilde{N} is the dominant component of DM, and N quanta from the gravitino decay make the main contribution to dark radiation. The corresponding decay width is given by Eq. (6), where $M_N \approx 1$ GeV.

For $m_{\tilde{G}} \gg m_{\tilde{N}}$, Eqs. (6), (11), and (13) result in $\Delta N_{\text{eff}} \propto m_{\tilde{G}}^{1/2}/m_{\tilde{N}}$. Therefore the $\Delta N_{\text{eff}} = \text{const}$ bands lie along the curves $m_{\tilde{N}}^2 \propto \Delta N_{\text{eff}}^{-2}/m_{\tilde{G}}$. Along this curve,

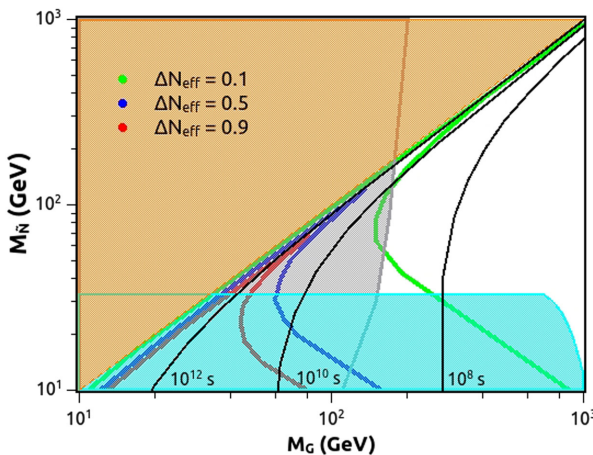


FIG. 6 (color online). The same as Fig. 4, but for case 3 ($\tilde{G} \rightarrow \tilde{N} + N$, $m_{\tilde{N}} \gg M_N \approx 1$ GeV).

$m_{\tilde{N}}/m_{\tilde{G}}$ decreases as $m_{\tilde{G}}$ becomes smaller. Hence, in order for the decay to be kinematically allowed, the $\Delta N_{\text{eff}} = \text{const}$ bands should eventually bend to the right. On the other hand, when $m_{\tilde{N}} \approx m_{\tilde{G}}$, we have $\Delta N_{\text{eff}} \propto 1/m_{\tilde{G}}^{1/2}(m_{\tilde{G}} - m_{\tilde{N}})$. This implies that the $\Delta N_{\text{eff}} = \text{const}$ bands join together around the $m_{\tilde{N}} = m_{\tilde{G}}$ line after turning to the right, as seen in the figure.

We find that the Lyman-alpha forest data is effective in constraining the parameter space for $m_{\tilde{G}} < 150$ GeV, while the galaxy power spectrum sets a stronger constraint for $m_{\tilde{N}} < 100$ GeV. Combining both constraints, we find that $\Delta N_{\text{eff}} \lesssim 0.5$ in the allowed region of the parameter space.

VII. CONCLUSION

In this work, we investigated a simple extension of the MSSM that accommodates late invisible decays to and of the gravitino. The model includes the new isosinglet color-triplet superfields X and \bar{X} and a singlet superfield N . Such an extension allows us to explain the baryon asymmetry of the Universe, and it can also address the DM-baryon coincidence puzzle. In addition to the LSP, this model has an R -parity even DM candidate when the singlet fermion N has $\mathcal{O}(\text{GeV})$ mass.

Interesting cases arise when the singlet scalar \tilde{N} and the gravitino \tilde{G} are the NLSP and the LSP, respectively, and vice versa. The resulting decays $\tilde{N} \rightarrow \tilde{G} + N$ and $\tilde{G} \rightarrow \tilde{N} + N$ have long lifetimes, as they involve gravitationally suppressed interactions. However, since both of the outgoing particles are invisible, these late decays are not subject to the tight BBN and CMB constraints on the hadronic and electromagnetic channels. On the other hand, depending on the mass ratios of the daughter and parent particles, it is possible that one or both of the DM candidates contribute to the amount of dark radiation or suppress perturbations at scales that are being probed by the galaxy power spectrum and the Lyman-alpha forest data. We performed a detailed study of the $m_{\tilde{N}} - m_{\tilde{G}}$ parameter space in light of these constraints and showed that the entire DM content of the Universe can be produced from the late invisible decays to and of the gravitino. Such decays have very important consequences in a broader context, as they considerably relax the constraints on the reheating of the Universe in SUSY models.

ACKNOWLEDGMENTS

We would like to thank Yu Gao for the helpful discussions. The work of R. A. is supported in part by NSF Grant No. PHY-1417510. The work of B. D. is supported by U.S. DOE Grant No. DE-FG02-13ER42020. The work of L. E. S. and M. W. is supported in part by NSF Grant No. PHY-1417457. F. Q. is partly supported by U.S. DOE Award No. SC0010107 and the Brazilian National Council for Technological and Scientific Development (CNPq).

- [1] For a review on dark matter, see G. Bertone, D. Hooper, and J. Silk, Particle dark matter: Evidence, candidates and constraints, *Phys. Rep.* **405**, 279 (2005); G. Jungman, M. Kamionkowski, and K. Griest, Supersymmetric dark matter, *Phys. Rep.* **267**, 195 (1996); L. E. Strigari, Galactic searches for dark matter, *Phys. Rep.* **531**, 1 (2013).
- [2] For a detailed review on the gravitino and its interactions, see T. Moroi, Effects of the gravitino on the inflationary universe, [arXiv:hep-ph/9503210](https://arxiv.org/abs/hep-ph/9503210).
- [3] M. Kawasaki, K. Kohri, T. Moroi, and A. Yotsuyanagi, Big-bang nucleosynthesis and gravitino, *Phys. Rev. D* **78**, 065011 (2008).
- [4] R. H. Cyburt, J. Ellis, B. D. Fields, F. Luo, K. A. Olive, and V. C. Spanos, Nucleosynthesis constraints on a massive gravitino in neutralino dark matter scenarios, *J. Cosmol. Astropart. Phys.* **10** (2009) 021.
- [5] J. R. Ellis, G. B. Gelmini, J. L. Lopez, D. V. Nanopoulos, and S. Sarkar, Astrophysical constraints on massive unstable neutral relic particles, *Nucl. Phys.* **B373**, 399 (1992).
- [6] W. Hu and J. Silk, Thermalization Constraints and Spectral Distortions for Massive Unstable Relic Particles, *Phys. Rev. Lett.* **70**, 2661 (1993).
- [7] D. J. Fixsen, E. S. Cheng, J. M. Gales, J. C. Mather, R. A. Shafer, and E. L. Wright, The cosmic microwave background spectrum from the full COBE FIRAS data set, *Astrophys. J.* **473**, 576 (1996).
- [8] T. Kanzaki, M. Kawasaki, K. Kohri, and T. Moroi, Cosmological constraints on neutrino injection, *Phys. Rev. D* **76**, 105017 (2007).
- [9] F. S. Queiroz, K. Sinha, and W. Wester, Rich tapestry: Supersymmetric axions, dark radiation, and inflationary reheating, *Phys. Rev. D* **90**, 115009 (2014); A. Freitas, F. D. Steffen, N. Tajuddin, and D. Wyler, Axinos in cosmology and at colliders, *J. High Energy Phys.* **06** (2011) 036; K. J. Bae, H. Baer, E. J. Chun, and C. S. Shin, Mixed axion/gravitino dark matter from SUSY models with heavy axinos, [arXiv:1410.3857](https://arxiv.org/abs/1410.3857); H. Baer, K.-Y. Choi, J. E. Kim, and L. Roszkowski, Dark matter production in the early Universe: Beyond the thermal WIMP paradigm, *Phys. Rep.* **555**, 1 (2015); K. J. Bae, H. Baer, A. Lessa, and H. Serce, Coupled Boltzmann computation of mixed axion neutralino dark matter in the SUSY DFSZ axion model, *J. Cosmol. Astropart. Phys.* **10** (2014) 082.
- [10] R. Allahverdi, M. Cicoli, B. Dutta, and K. Sinha, Correlation between dark matter and dark radiation in string compactifications, *J. Cosmol. Astropart. Phys.* **10** (2014) 002; R. Allahverdi, M. Cicoli, B. Dutta, and K. Sinha, Nonthermal dark matter in string compactifications, *Phys. Rev. D* **88**, 095015 (2013); R. Allahverdi, B. Dutta, and K. Sinha, Nonthermal Higgsino dark matter: Cosmological motivations and implications for a 125 GeV Higgs, *Phys. Rev. D* **86**, 095016 (2012); B. Dutta, L. Leblond, and K. Sinha, Mirage in the sky: Nonthermal dark matter, gravitino problem, and cosmic ray anomalies, *Phys. Rev. D* **80**, 035014 (2009); R. Allahverdi, B. Dutta, and K. Sinha, Cladogenesis: Baryon-dark matter coincidence from branchings in moduli decay, *Phys. Rev. D* **83**, 083502 (2011).
- [11] R. Allahverdi, B. Dutta, and K. Sinha, Baryogenesis and late-decaying moduli, *Phys. Rev. D* **82**, 035004 (2010).
- [12] R. Allahverdi, B. Dutta, R. N. Mohapatra, and K. Sinha, Supersymmetric Model for Dark Matter and Baryogenesis Motivated by the Recent CDMS Result, *Phys. Rev. Lett.* **111**, 051302 (2013).
- [13] For recent reviews on reheating, see R. Allahverdi, R. Brandenberger, F.-Y. Cyr-Racine, and A. Mazumdar, Reheating in inflationary cosmology: Theory and applications, *Annu. Rev. Nucl. Part. Sci.* **60**, 27 (2010); M. A. Amin, M. P. Hertzberg, D. I. Kaiser, and J. Karouby, Nonperturbative dynamics of reheating after inflation: A review, *Int. J. Mod. Phys. D* **24**, 1530003 (2015).
- [14] K. S. Babu, R. N. Mohapatra, and S. Nasri, Unified TeV Scale Picture of Baryogenesis and Dark Matter, *Phys. Rev. Lett.* **98**, 161301 (2007).
- [15] M. Miura, *Proceedings of the 14th International Conference on Advanced Technology and Particle Physics Como, Italy, 23 - 27 September 2013*, 2011, pp. 275–279, http://www.worldscientific.com/doi/abs/10.1142/9789814603164_0042.
- [16] R. Allahverdi and B. Dutta, Natural GeV dark matter and the baryon-dark matter coincidence puzzle, *Phys. Rev. D* **88**, 023525 (2013).
- [17] B. Dutta, Y. Gao, and T. Kamon, Probing light nonthermal dark matter at the LHC, *Phys. Rev. D* **89**, 096009 (2014).
- [18] R. Allahverdi, B. Dutta, and Y. Gao, keV photon emission from light nonthermal dark matter, *Phys. Rev. D* **89**, 127305 (2014).
- [19] E. Behnke *et al.* (COUPP Collaboration), First dark matter search results from a 4-kg CF₃I bubble chamber operated in a deep underground site, *Phys. Rev. D* **86**, 052001 (2012); **90**, 079902(E) (2014).
- [20] P. J. Fox, R. Harnik, R. Primulando, and C.-T. Yu, Taking a razor to dark matter parameter space at the LHC, *Phys. Rev. D* **86**, 015010 (2012); A. Rajaraman, W. Shepherd, T. M. P. Tait, and A. M. Wijangco, LHC bounds on interactions of dark matter, *Phys. Rev. D* **84**, 095013 (2011).
- [21] D. S. Akerib *et al.* (LUX Collaboration), First Results from the LUX Dark Matter Experiment at the Sanford Underground Research Facility, *Phys. Rev. Lett.* **112**, 091303 (2014).
- [22] P. Graf and F. D. Steffen, Dark radiation and dark matter in supersymmetric axion models with high reheating temperature, *J. Cosmol. Astropart. Phys.* **12** (2013) 047; A. Freitas, F. D. Steffen, N. Tajuddin, and D. Wyler, Axinos in cosmology and at colliders, *J. High Energy Phys.* **06** (2011) 036.
- [23] P. A. R. Ade *et al.* (Planck Collaboration), Planck 2013 results. XVI. Cosmological parameters, *Astron. Astrophys.* **571**, A16 (2014).
- [24] A. G. Riess, L. Macri, S. Casertano, H. Lampeitl, H. C. Ferguson, A. V. Filippenko, S. W. Jha, W. Li, and R. Chornock, A 3% solution: Determination of the Hubble constant with the Hubble space telescope and wide field camera 3, *Astrophys. J.* **730**, 119 (2011); **732**, 129(E) (2011).
- [25] M. Wyman, D. H. Rudd, R. A. Vanderveld, and W. Hu, $\nu\Lambda$ CDM: Neutrinos Help Reconcile Planck with the Local Universe, *Phys. Rev. Lett.* **112**, 051302 (2014).

- [26] P. A. R. Ade *et al.* (BICEP2 Collaboration), Detection of B-Mode Polarization at Degree Angular Scales by BICEP2, *Phys. Rev. Lett.* **112**, 241101 (2014).
- [27] C. Dvorkin, M. Wyman, D. H. Rudd, and W. Hu, Neutrinos help reconcile Planck measurements with both early and local Universe, *Phys. Rev. D* **90**, 083503 (2014); J.-F. Zhang, Y.-H. Li, and X. Zhang, Cosmological constraints on neutrinos after BICEP2, *Eur. Phys. J. C* **74**, 2954 (2014).
- [28] D. Hooper, F. S. Queiroz, and N. Y. Gnedin, Nonthermal dark matter mimicking an additional neutrino species in the early Universe, *Phys. Rev. D* **85**, 063513 (2012).
- [29] C. Kelso, S. Profumo, and F. S. Queiroz, Nonthermal WIMPs as “dark radiation” in light of ATACAMA, SPT, WMAP9, and Planck, *Phys. Rev. D* **88**, 023511 (2013).
- [30] C. Kelso, C. A. de S. Pires, S. Profumo, F. S. Queiroz, and P. S. Rodrigues da Silva, A 331 WIMPy dark radiation model, *Eur. Phys. J. C* **74**, 2797 (2014).
- [31] F. S. Queiroz, Non-thermal WIMPs as dark radiation, *AIP Conf. Proc.* **1604**, 83 (2014).
- [32] S. Roychowdhury, J. N. Chengalur, A. Begum, and I. D. Karachentsev, Thick gas discs in faint dwarf galaxies, *Mon. Not. R. Astron. Soc.* **404**, L60 (2010); G.-B. Zhao, S. Saito, W. J. Percival, A. J. Ross, F. Montesano, M. Viel, D. P. Schneider, M. Manera, J. Miralda-Escude, N. Palanque-Delabrouille *et al.*, The clustering of galaxies in the SDSS-III Baryon Oscillation Spectroscopic Survey: Weighing the neutrino mass using the galaxy power spectrum of the CMASS sample, *Mon. Not. R. Astron. Soc.* **436**, 2038 (2013).
- [33] P. McDonald *et al.*, The Lyman-alpha forest power spectrum from the Sloan Digital Sky Survey, *Astrophys. J. Suppl. Ser.* **163**, 80 (2006).
- [34] N. Palanque-Delabrouille *et al.*, The one-dimensional Ly-alpha forest power spectrum from BOSS, *Astron. Astrophys.* **559**, A85 (2013).
- [35] A. Boyarsky, J. Lesgourgues, O. Ruchayskiy, and M. Viel, Lyman-alpha constraints on warm and on warm-plus-cold dark matter models, *J. Cosmol. Astropart. Phys.* **05** (2009) 012.
- [36] M. Kaplinghat, Dark matter from early decays, *Phys. Rev. D* **72**, 063510 (2005).
- [37] L. E. Strigari, M. Kaplinghat, and J. S. Bullock, Dark matter halos with cores from hierarchical structure formation, *Phys. Rev. D* **75**, 061303 (2007).